Leisenheimer, Leonie; Wellmann, Thilo; Jänicke, Clemens; Haase, Dagmar

Monitoring drought impacts on street trees using remote sensing - Disentangling temporal and species-specific response patterns with Sentinel-2 imagery

Ecological Informatics

Provided in Cooperation with:
Leibniz Institute of Agricultural Development in Transition Economies (IAMO), Halle (Saale)

Suggested Citation: Leisenheimer, Leonie; Wellmann, Thilo; Jänicke, Clemens; Haase, Dagmar (2024) : Monitoring drought impacts on street trees using remote sensing - Disentangling temporal and species-specific response patterns with Sentinel-2 imagery, Ecological Informatics, ISSN 1878-0512, Elsevier, Amsterdam, Vol. 82, pp. 1-14, https://doi.org/10.1016/j.ecoinf.2024.102659 , https://www.sciencedirect.com/science/article/pii/S1574954124002012

This Version is available at:
https://hdl.handle.net/10419/299787

Ecological Informatics 82 (2024) 102659

Contents lists available at ScienceDirect

Ecological Informatics

journal homepage: www.elsevier.com/locate/ecolinf

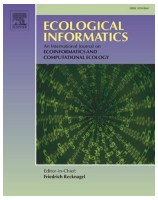

Monitoring drought impacts on street trees using remote sensing - Disentangling temporal and species-specific response patterns with Sentinel-2 imagery

Leonie Leisenheimer [a], Thilo Wellmann [a,*], Clemens Jänicke [b,a,c], Dagmar Haase [a,d]

[a] Humboldt-Universität zu Berlin, Geography Department, 10099 Berlin, Germany
[b] Leibniz Institute of Agricultural Development in Transitions Economies (IAMO), 06120 Halle (Saale), Germany
[c] Integrative Research Institute on Transformations of Human-Environment Systems, Humboldt-Universität zu Berlin, Geography Department, 10099 Berlin, Germany
[d] Helmholtz Centre for Environmental Research – UFZ, Department of Computational Landscape Ecology, 04318 Leipzig, Germany

ARTICLE INFO

Keywords:
Green infrastructure
Urban tree health
Earth observation time series
Vegetation indices
Land surface phenology
Compact city of Leipzig

ABSTRACT

Healthy street trees provide important ecosystem services to cities, but are under increasing stress from urbanisation and climate change, including drought. Traditional field observations are limited in their ability to provide city-wide and regular monitoring of the drought response of street trees, which is essential for their effective management. To overcome this, we propose a novel workflow using freely available remote sensing imagery from Sentinel-2 to identify temporal and species-specific drought response patterns of street trees. We evaluate the workflow on a sample of 2514 mature street trees of the seven most common street tree species in Leipzig, Germany. For each tree, we generate time series of eight vegetation indices from 2017 to 2022, namely enhanced vegetation index (EVI), normalised burn ratio (NBR) and normalised difference vegetation index (NDVI), each using the 10 m and 20 m resolution near-infrared band (EVI-10, EVI-20, NBR-10, NBR-20, NDVI-10, NDVI-20), as well as red edge normalised difference vegetation index (RENDVI) and red-green vegetation index (RGVI). They form the basis for a correlation analysis with the meteorological drought indicator standardised precipitation evapotranspiration index (SPEI) and for annual growing season integrals, which we subtract from those of the base year 2017. We use boxplots and statistical hypothesis testing to examine differences between and within tree species and years. The results show positive relationships between the eight vegetation indices and the SPEI, with the NBR-20 having the highest correlation coefficients. We also find significant differences in the drought response of several tree species, with *Quercus robur* being the most drought responsive and *Platanus x acerifolia* being the least. While most tree species have significantly smaller growing season integrals in the drought years 2018 and 2020 than in the non-drought years 2017 and 2021, the effects are not as pronounced in the drought years 2019 and 2022. Uncertainties arise, for example, from spectral signal variations caused by adjacent land use. Nevertheless, the proposed workflow holds promise for incorporation into holistic urban green management solutions and mixed-method approaches for further research into the causes and consequences of drought-induced damage to street trees.

1. Introduction

The responses of urban vegetation to drought are as diverse as the temporal scales of the phenomenon (Miller et al., 2022), complicating the study of drought response patterns. Droughts are extreme events of insufficient moisture conditions due to precipitation deficits. Unlike some other extreme events, the phenomenon and its effects extend over multiple time scales and occur gradually (Gessner et al., 2013; Pluntke et al., 2021; Zhao et al., 2020). This study focuses on meteorological droughts, which result from a negative water balance due to reduced precipitation and increased evapotranspiration for a given period and region compared to the long-term average (Bernhofer et al., 2015). In contrast, agricultural and hydrological droughts include additional factors that influence moisture conditions, such as soil moisture, groundwater, streamflow, and surface water storage (Jiao et al., 2021). Thus, the timing, duration, and magnitude of droughts depend on both the accumulation period of moisture deficits and the factors considered according to the drought definition (Bernhofer et al., 2015).

* Corresponding author.

https://doi.org/10.1016/j.ecoinf.2024.102659
Received 20 November 2023; Received in revised form 29 May 2024; Accepted 31 May 2024
Available online 3 June 2024

Monitoring the effects of drought on vegetation is increasingly relevant because healthy urban vegetation provides important ecosystem services to cities and their inhabitants, such as heat mitigation, noise buffering, and space for recreation (Kabisch et al., 2021; Kraemer and Kabisch, 2022; Rey-Gozalo et al., 2023). The need for such services is increasing due to the ongoing trends of urbanisation and climate change. At the same time, however, urban vegetation itself is affected by several threats caused by these trends such as poor air quality, sealed surfaces, and droughts. These stresses ultimately reduce the needed ecosystem services of urban vegetation (Cârlan et al., 2020; Kabisch et al., 2021).

Street trees, as part of the urban vegetation, are particularly exposed to these threats (Haase and Hellwig, 2022). Impervious surfaces and the urban heat island can increase water and heat stress on street trees (Mullaney et al., 2015). Knowledge of the stress response patterns of street trees could improve the management of urban green spaces and hence the provision of ecosystem services (Fang et al., 2020). Traditionally, costly and labour-intensive field observations are used to monitor the health of street trees, but they are not feasible for larger areas and regular observations (Ciesielski and Sterenczak, 2019; García-Pardo et al., 2022; Haase and Hellwig, 2022). Publicly available remote sensing imagery provides an alternative for citywide and regular assessment of the street tree health.

Remote sensing images are already widely used for urban studies, but the opportunities offered by dense time series are often missed. For example, some studies map urban green spaces and classify urban vegetation (Aryal et al., 2022; Duarte et al., 2014; Kopecká et al., 2017), while others study urban-rural gradients and heat island effects (Krehbiel et al., 2016; Qiu et al., 2020). However, most studies focus on large areas rather than small features such as street trees, and often do not exploit the temporal information of remote sensing times series (Shahtahmassebi et al., 2021). Therefore, land surface phenology is understudied in urban areas (Jochner and Menzel, 2015; Krehbiel et al., 2016; Qiu et al., 2020), although it is well suited to differentiate vegetation responses to climate impacts, such as drought, as well as inter- and intra-annual land cover changes, including vegetation disturbance and recovery (Brooks et al., 2020; Jochner and Menzel, 2015; Zeng et al., 2020). Recent advances in the spatial, radiometric, spectral, and temporal resolution of remote sensing imagery hold great promise for conducting such intra-annual analyses in heterogeneous urban environments (García-Pardo et al., 2022; Wellmann et al., 2020; Zhu et al., 2019).

Sentinel-2 provides freely accessible multispectral optical data with a spatial resolution of ten metres and a temporal revisit time of five days (ESA, 2023). The main objective of this study is to develop a workflow that uses Sentinel-2 derived vegetation indices[1] and drought response metrics from 2017 to 2022 to describe the impact of a multi-year drought on prevalent mature street trees in Leipzig, Germany. Specifically, we address and answer the following research questions:

(1) How do different vegetation indices relate to meteorological drought conditions?
(2) What temporal and species-specific drought response patterns of street trees does the correlation between meteorological drought conditions and vegetation indices reveal?
(3) What temporal and species-specific drought response patterns of street trees do growing season integrals of vegetation index time series reveal?

We address these questions by using time series analysis, correlation analysis, land surface phenology analysis, and statistical hypothesis testing. For the first and second research questions, we examine the relationship between meteorological drought conditions and vegetation indices using Pearson's correlation coefficient to compare eight vegetation indices and to identify the cumulative effects of drought on different tree species. Based on the comparison of vegetation indices, we select the index with the highest correlation for research questions two and three. Within the third research question, we calculate annual growing season integrals of the vegetation index time series. Here, we focus on interannual variations in the drought response of the street trees studied. Quantitative validation of time series is difficult due to a lack of ground-truthing data (Löw and Koukal, 2020). Therefore, we evaluate the validity and information content of the developed drought response metrics based on the timing of drought events in Leipzig between 2017 and 2022 and on the drought tolerance of the studied tree species. These are *Platanus x acerifolia* (*P. x acerifolia*), *Quercus robur* (*Q. robur*), *Tilia cordata* (*T. cordata*), *Fraxinus excelsior* (*F. excelsior*), *Aesculus hippocastanum* (*A. hippocastanum*), *Acer pseudoplatanus* (*A. pseudoplatanus*), and *Acer platanoides* (*A. platanoides*).

1.1. Effect of droughts on common street tree species

A common response of trees to drought is to close the stomata to reduce water loss, resulting in lower photosynthetic rates and reduced ecosystem services such as carbon uptake. In the medium term, trees respond by deforming their leaves and dropping leaves or whole branches. In the long term, mortality increases, growth is reduced and shorter shoots are formed (Brune, 2016).

The drought response of trees depends on the duration and severity of the drought and varies between species. Due to different morphological and physiological characteristics, some species are more drought tolerant than others (Table 1). In general, spring water availability strongly influences tree health (Hirsch et al., 2023; Moser et al., 2017). Some trees, such as *P. x acerifolia* and *A. platanoides*, respond to water deficits with a time lag, resulting in limited growth in the years following the drought (Gillner et al., 2014; Hirsch et al., 2023).

Table 1
Drought tolerance of common street tree species based on core literature about (urban street) tree properties, bio-physical tolerances and sensitivities including water requirements, leaf area index, insolation resistance and stomata properties (Hessisches Landesamt für Naturschutz, Umwelt und Geologie [HLNUG], 2023; Roloff et al., 2009; TU Dresden, 2015).

Tree species \ Source	TU Dresden, 2015	Roloff et al., 2009	HLNUG, 2023	Brune, 2016	Hirsch et al., 2023
Platanus x acerifolia	very tolerant	very suitable	good		less affected by drought
Quercus robur	sensitive	problematic	medium	moderately tolerant	less affected by drought
Tilia cordata	drought tolerant	suitable	medium		particularly sensitive to drought
Fraxinus excelsior	drought tolerant	suitable	medium	moderately tolerant	
Aesculus hippocastanum	not drought tolerant	not very suitable	low	moderately sensitive	
Acer pseudoplatanus	not drought tolerant	not very suitable		moderately sensitive	
Acer platanoides	drought tolerant	suitable	medium	moderately tolerant	particularly sensitive to drought

Legend: most drought tolerant ... least drought tolerant, no data

[1] EVI-10, EVI-20, NBR-10, NBR-20, NDVI-10, NDVI-20, RENDVI, and RGVI

1.2. Remote sensing analysis for urban street tree monitoring

Despite recent advances in remote sensing sensors, accurate monitoring of the response of street trees to drought remains challenging. Spectral signals are affected by heterogeneous urban land cover, leading to mixed pixel problems, mistaking bright surfaces for clouds and snow, and altering shaded areas (García-Pardo et al., 2022; Haase et al., 2019; van der Linden et al., 2019; Zhu et al., 2019). As droughts and vegetation dynamics occur at different temporal scales, the processes need to be disentangled. For example, drought-induced damage occurs in addition to long-term trends, the seasonal cycle and random fluctuations. Remote sensing analysis for street tree monitoring thus faces the problem of decomposing additive time series in a setting of heterogeneous, spectrally ambiguous urban land cover.

The literature on monitoring the health of street trees using remote sensing data is modest, but key studies analysing the health of individual street trees are: Fang et al. (2020), who develop a classification model to distinguish between health classes, and Granero-Belinchon et al. (2020), who develop a reconstruction methodology for vegetation index time series in urban areas. Both studies focus on trees with a large crown size by masking non-vegetated pixels based on a vegetation index threshold and a previous classification, respectively. For our study, Miller et al. (2022) and Löw and Koukal (2020) are key publications from a methodological perspective. Miller et al. (2022) investigate the temporal dimension of drought responses by correlating drought indices calculated over different time periods, i.e. the SPEI, with the NDVI and the difference in land surface temperature (LST) between vegetation and impervious surfaces. They compare the correlation results between spatially aggregated patches of broadleaf, needleleaf, eucalyptus and oak trees, as well as annual grasses and turfgrass lawns. Löw and Koukal (2020) assess temporal patterns of drought response by subtracting the time series of a detection period from a reference time series. This approach is similar to the vegetation condition index (VCI), which compares the vegetation index value of a given year to the maximum vegetation index value of reference time series from the same location (Kogan, 1990). A pixel-based analysis makes these approaches applicable to urban areas. The correlation analysis of Miller et al. (2020) and the time series deviations of Löw and Koukal (2020) form the basis of the drought response metrics developed here.

At the patch level, Cârlan et al. (2020) build a linear mixed-effect model that shows that irrigation systems, LST, and distance to lakes and roads are the main drivers of vegetation conditions. Li et al. (2017) decompose a three-year time series, which allows them to identify seasonal patterns and long-term trends, such as the greening of broadleaf trees between 2010 and 2013, and fewer intra-annual disturbances due to heat compared to shrubs (Li et al., 2017). The above studies demonstrate the feasibility of remotely sensed monitoring of street tree health, while also highlighting its limitations – including filtering for mature trees, masking non-vegetated pixels, and applying strict outlier exclusion criteria.

2. Methodology

2.1. Study area

Leipzig is a fast-growing city in central Germany with an average annual rainfall of 611 mm (Deutscher Wetterdienst [DWD], 2023) (Fig. 1). The city experienced multiple drought events in the past years with 2018, 2019, 2020, and 2022 being the warmest on record (Fuchs, 2022; Imbery et al., 2023). Although 2021 was slightly wetter and

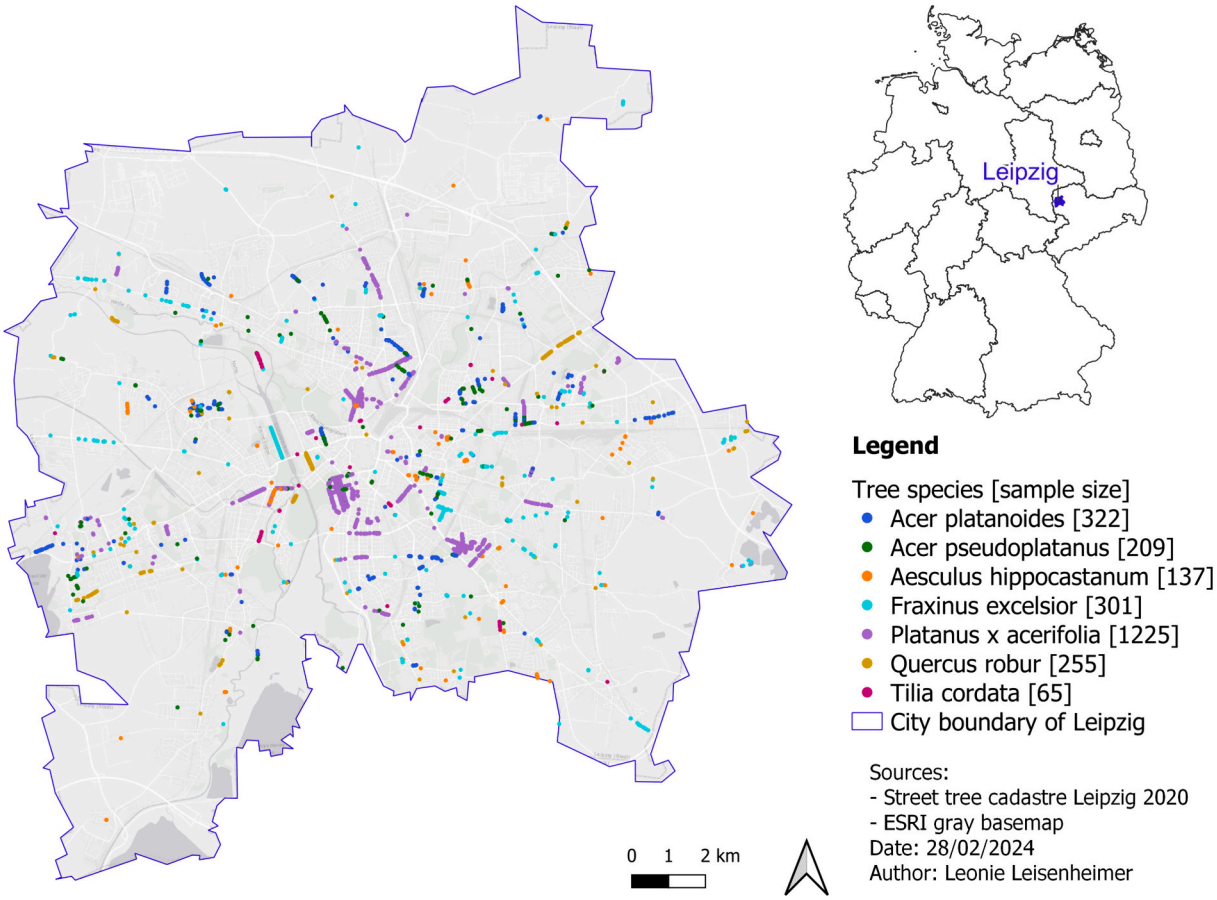

Fig. 1. Map of the city of Leipzig and the street tree sample by tree species.

cooler, the meteorological drought of the previous years resulted in the most severe groundwater drought in 100 years (Fuchs, 2022). It is projected that droughts will occur more often in Leipzig with an estimated 34% decrease in summer precipitation coupled with 3.7 to 5.4 °C increase in annual temperature by 2071 (Rumpf, 2021a, 2021b).

Leipzig's climate adaptation strategy defines urban trees as an important measure to mitigate heat, especially through shading (Stadt Leipzig, 2021). At the same time, the city recognises the many threats to street trees, which affect older trees in particular, as the prolonged drought of recent years has dried out deeper layers of soil (Stadt Leipzig, 2019a). Irrigation is mainly used for young trees up to ten years of age. In addition, citizens are motivated to contribute by adopting and watering young trees (Stadt Leipzig, 2023). The city of Leipzig identifies a potential of 45,000 additional street trees, aiming to plant 1000 trees a year (Stadt Leipzig, 2019b).

2.2. Data and its processing

2.2.1. Climate data for characterizing drought conditions

In this study, we use the monthly sum of precipitation and the monthly mean temperature from the weather station "Leipzig-Holzhausen" from January 1991 to December 2022 (Deutscher Wetterdienst [DWD], 2023) as reference climate data. They serve as input to calculate the drought indicator standardised precipitation evapotranspiration index (SPEI) for which we use the R-package "SPEI" (Fig. 2) (Beguería and Vicente-Serrano, 2023). The SPEI quantifies the deviation from the average water balance, with values below −1 being defined as drought (Li et al., 2015; Pluntke et al., 2021). SPEI is a widely used indicator in studies on vegetation response to drought (Li et al., 2015; Mazza et al., 2021; Miller et al., 2022; Zhao et al., 2020). We follow the scheme of Thornthwaite to compute the potential evapotranspiration and the climatic water balance using the temperature and precipitation data as an intermediate step as described by Vicente-Serrano et al. (2010) and implemented in the R-package "SPEI" (Beguería and Vicente-Serrano, 2023). The water balance is calculated over a certain number of previous months. Within this study, we use periods of 1, 3, 6, 9, 12, and 24 months – named SPEI-1, SPEI-3, SPEI-6, SPEI-9, SPEI-12, and SPEI-24, respectively – to account for intra-annual as well as inter-annual drought effects. The calculation (Appendix 1.1) indicates that 2017 and 2021 are hardly affected by drought across all SPEI periods, thus hereafter referred to as non-drought years. We label the other years (i.e., 2018, 2019, 2020, 2022) as drought years.

2.2.2. Tree sampling based on Leipzig's street tree cadastre

Leipzig's street tree cadastre lists 60,000 street trees (Stadt Leipzig, 2019b, 2020). It contains information on tree species, age, location, crown diameter, and site characteristics, with the latter two not being available publicly (Stadt Leipzig, 2020). Among the street trees with a crown diameter greater than ten metres, the species *P. x acerifolia*, *Q. robur*, *T. cordata*, *F. excelsior*, *A. hippocastanum*, *A. pseudoplatanus*, and

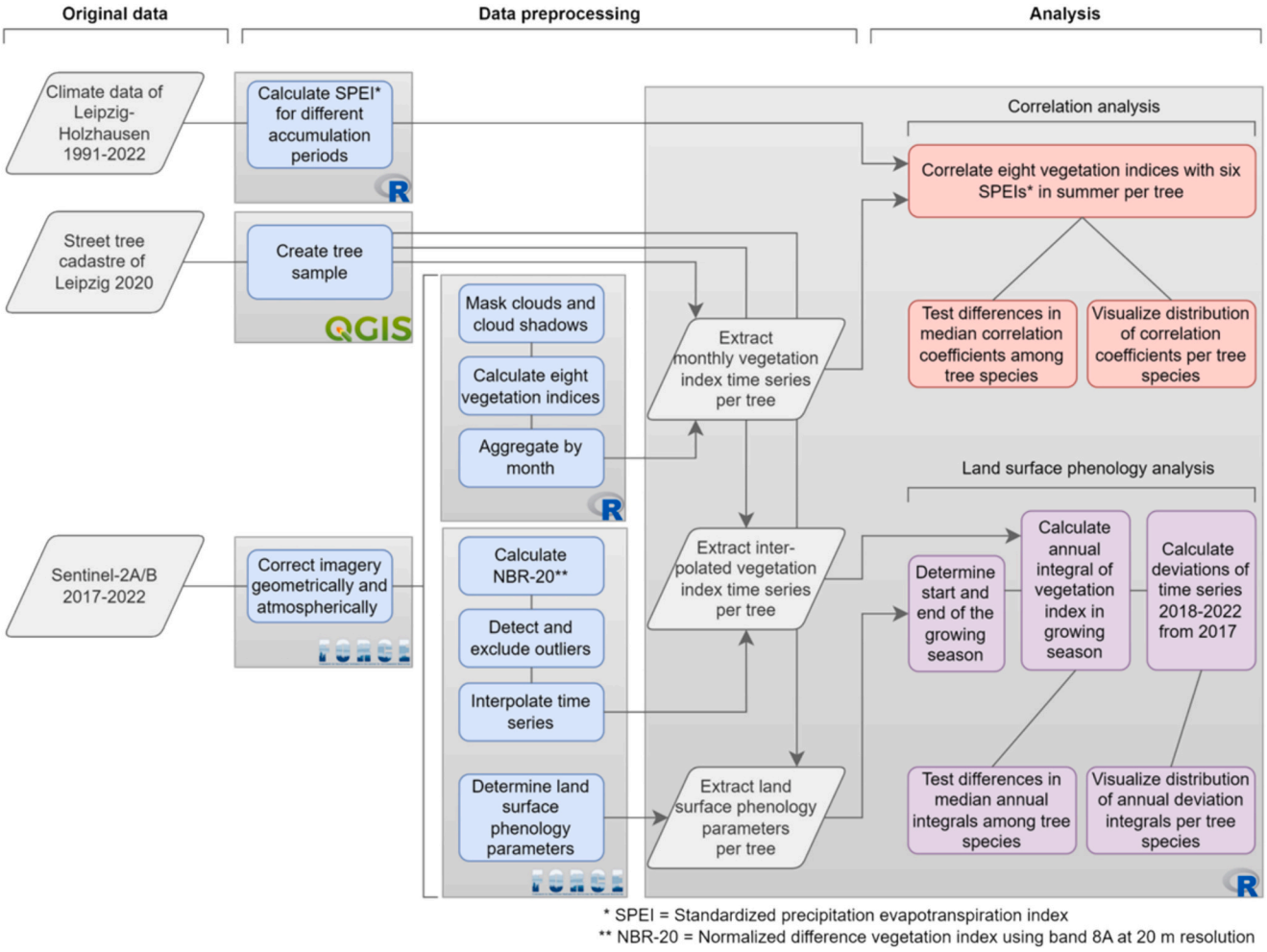

Fig. 2. Schematic workflow. The correlation analysis (coloured in red) is the basis for research questions (1) and (2), while the land surface phenology analysis (coloured in purple) is used for research question (3). (For interpretation of the references to color in this figure legend, the reader is referred to the web version of this article.)

A. platanoides dominate with a total share of 45%. These species have at least 250 individuals with a crown diameter of at least ten metres (Appendix 1.2).

We derive a sample of trees suitable for analysis with Sentinel-2 imagery by first selecting only street trees. Then we select trees with crown diameters greater than ten metres that cover at least 50% of a Sentinel-2 pixel to ensure a high spectral signal from the tree. Among these, we additionally exclude trees whose crowns overlap in the same pixels, to reduce spectral mixtures of neighbouring trees. To do so, we buffer the locations of the street trees in the geographic information system (GIS) software QGIS with the crown radius and filter the trees based on Sentinel-2 overlaps. This procedure yields 2514 individual trees (Fig. 1).

2.2.3. Vegetation index time series reconstruction with Sentinel-2 imagery

Since 2017, the Sentinel-2 satellites provide imagery of Leipzig with a temporal resolution of five days, including 13 spectral bands with resolutions of 10, 20 and 60 m (Granero-Belinchon et al., 2020). We use all imagery between 2017 and 2022 with up to 90% cloud cover, processed with the "framework for operational radiometric correction for environmental monitoring" (FORCE) software (Frantz, 2019). During the pre-processing of the original Sentinel-2 data in FORCE, the 20 m bands are transformed to 10 m resolution using the ImproPhe algorithm (Frantz et al., 2016). The processing additionally includes radiometric and geometric correction, outlier detection, and time series interpolation (Frantz, 2019). Cloud detection is performed using the Fmask algorithm, and images are geometrically co-registered with Landsat imagery to account for inaccuracies in early Sentinel-2 imagery (Appendix 1.3).

To monitor vegetation health, we use vegetation indices that have been shown to be valuable for analysing tree health in urban areas (Table 2). Vegetation indices correlate with leaf water content, canopy structure, and chlorophyll content (Chuvieco, 2020; Fang et al., 2020). For instance, while photosynthetically active vegetation has a low reflectance in the red band and high reflectance in the near-infrared band, stressed vegetation shows the opposite pattern, which is captured by the NDVI and EVI (Chuvieco, 2020). By combining different reflectance bands, the selected indices relate to different tree traits and therefore have their distinct advantages and disadvantages. The NBR, as the only water-related vegetation index in this study, is better suited for determining canopy water content than the other indices (Miller et al., 2020). The NDVI stands out due to its sensitivity to sparse vegetation and its widespread usage (Chuvieco, 2020). The EVI reduces soil, aerosol, and saturation effects compared to NDVI by additionally incorporating a canopy background adjustment factor and the blue band (Chuvieco, 2020). The RENDVI is able to capture the density of tree canopies, and the RGVI is particularly sensitive to wilting (Guzmán et al., 2023; Misra et al., 2016).

We generate two distinct time series of vegetation indices. The first time series is derived from bottom-of-atmosphere reflectance imagery and quality assurance information (QAI) provided by FORCE. Based on this QAI, we exclude all pixels flagged as clouds, cloud shadows, snow, saturated, and below freezing temperatures (Frantz, 2019). We then calculate the selected vegetation indices using the formulas provided in Table 2 and aggregate them on a monthly basis. The aggregation relies on the median vegetation index for each month, as it is more robust to extreme values than the mean (Miller et al., 2022). In some months, there are no suitable observations, which leads to data gaps in the time series. The second time series is further processed using the time series analysis module of FORCE for the NBR-20. The time series module uses radial basis filter ensembles for the outlier detection and exclusion, as well as interpolation and smoothing of the time series as described by Schwieder et al. (2016). We interpolate the time series to a dense 16-days-sample. For each interpolation step, all observations with a time interval of 16 days are considered. Thus, this second time series overcomes the drawback of potential data gaps but is only computed for the NBR-20.

Table 2
Vegetation indices used in this study. The wavelengths listed in the table represent the central wavelengths of the respective bands in the Sentinel-2 sensor.

Index	Name	Equation (central wavelengths)	Original resolution	References
NDVI-10	Normalised Difference Vegetation Index (using broad NIR band at 10 m resolution)	(842 nm - 665 nm) / (842 nm + 665 nm)	10 m	Tucker, 1979; Granero-Belinchon et al., 2020; Löw and Koukal, 2020
NDVI-20	Normalised Difference Vegetation Index (using narrow NIR band at 20 m resolution)	(865 nm - 665 nm) / (865 nm + 665 nm)	20 m	Tucker, 1979; Cärlan et al., 2020
EVI-10	Enhanced Vegetation Index (using broad NIR band at 10 m resolution)	2.5 * ((842 nm - 665 nm) / (842 nm + 6 * 665 nm – 7.5 * 490 nm + 1))	10 m	Huete et al., 2002; Nagler et al., 2005
EVI-20	Enhanced Vegetation Index (using narrow NIR band at 20 m resolution)	2.5 * ((865 nm - 665 nm) / (865 nm + 6 * 665 nm – 7.5 * 490 nm + 1))	20 m	Huete et al., 2002
NBR-10	Normalised Burn Ratio (using broad NIR band at 10 m resolution)	(842 nm - 2190 nm) / (842 nm + 2190 nm)	20 m	Key and Benson, 2006
NBR-20	Normalised Burn Ratio (using narrow NIR band at 20 m resolution)	(865 nm - 2190 nm) / (865 nm + 2190 nm)	20 m	Key and Benson, 2006; Granero-Belinchon et al., 2020
RENDVI	Red Edge Normalised Difference Vegetation Index	(740 nm - 705 nm) / (740 nm + 705 nm)	20 m	Gitelson and Merzlyak, 1994; Cärlan et al., 2020; Granero-Belinchon et al., 2020
RGVI	Red-Green Vegetation Index	(560 nm - 665 nm) / (560 nm + 665 nm) + 0.5	10 m	Motohka et al., 2010; Fang et al., 2020; Löw and Koukal, 2020

Annual land surface phenology parameters are computed by FORCE based on a polar coordinate transformation of the vegetation index time series (Brooks et al., 2020). Land surface phenology describes seasonal patterns in the phenological phases of plants and can be derived from remotely sensed time series of vegetation indices (Caparros-Santiago et al., 2021; Duarte et al., 2014). We use the parameters start and end of the season.

2.3. Methods for drought response analysis

Vegetation indices serve as proxies for biophysical variables such as photosynthesis, biomass, and green vegetation fraction (Chuvieco, 2020). However, their absolute values lack explanatory power, especially when assessing urban street trees. First, vegetation indices do not directly measure biophysical variables and therefore cannot identify the underlying causes of changes in greenness (Chuvieco, 2020). Second, the fractional tree cover within pixels can vary due to the heterogeneity of urban surfaces. For instance, low vegetation index values do not

necessarily indicate unhealthy vegetation, as low values could come from other land cover, such as bare soil. Consequently, the shape, rather than the magnitude, of the vegetation index time series becomes critical in describing drought response (Fang et al., 2020). To address this, we develop two drought response metrics for each tree, as described in the following sections and in Appendix 1.4 using an example tree.

2.3.1. Correlation coefficients as indicators for drought response

Correlation analysis stands out for its ability to reveal temporal drought response patterns, especially cumulative and time-lagged effects (Zhao et al., 2020). Therefore, it is a common approach in analysing drought responses of trees in remote sensing studies (Gessner et al., 2013; Jain et al., 2010; Ji and Peters, 2003; Li et al., 2015; Miller et al., 2022; Zhao et al., 2020). Strong positive correlations between drought and vegetation indices indicate a high sensitivity of vegetation to drought (Gessner et al., 2013).

Following Gessner et al. (2013) and Miller et al. (2022), we apply a pixel-based linear correlation approach. We only include the summer months of June, July, and August because these months have shown the highest correlation coefficients in previous studies (Gillner et al., 2015; Ji and Peters, 2003; Mazza et al., 2021; Miller et al., 2022). We calculate Pearson's correlation coefficients for all possible combinations of the six SPEI periods (Section 2.2.1) and eight vegetation indices (Table 2) of the monthly aggregated time series for each tree. The dimensionless Pearson's correlation coefficient is suitable for linear relationships between metrically scaled variables (Mittag, 2017) and has been widely used to assess such interactions (Gillner et al., 2014; Li et al., 2015; Mazza et al., 2021).

We explore differences in correlation coefficients between tree species, accumulation periods, and vegetation indices using descriptive statistics and hypothesis tests. We choose non-parametric pairwise Wilcoxon tests to assess the significance of differences, as homoscedasticity and normally distributed residuals are not given (Crawley, 2013).

2.3.2. Land surface phenology parameters as indicators for drought response

As a second metric of drought response, we compute growing season integrals to indicate seasonal vegetation productivity (Borgogno-Mondino and Fissore, 2022; Li et al., 2017). Löw and Koukal (2020) suggest that the integrals reflect both the severity and the duration of disturbance events. Following Borgogno-Mondino and Fissore (2022), annual integrals are defined as the sum of daily vegetation indices from the beginning to the end of the season, calculated for each year. For the calculation we use the interpolated NBR-20 time series provided by FORCE. We linearly interpolate this time series to obtain daily values. We choose a fixed period for the growing season to ensure comparability between years, using the year 2017 as it is hardly affected by any drought (Appendix 1.1). This defines the beginning and end of the growing season as day of the year 133 and 280, respectively.

As the absolute growing season integrals lack in their meaningfulness, we adapt the approach by Löw and Koukal (2020), who calculate deviations between the integral of a detection period and a baseline (Eq. (1)). In our study, the detection period is represented by the years 2018 to 2022, respectively, and the baseline by 2017.

$$\text{Deviation integral} = \sum_{t=SOS}^{EOS} BL_t - DP_t \quad (1)$$

where SOS = start of the season, EOS = end of the season, BL = baseline, DP = detection period, t = time.

Similar to the analysis of correlation coefficients, we use the deviation integrals to analyse temporal and species-specific patterns. Differences in inter-annual drought responses are tested for significance with pairwise Wilcoxon tests. For the test, we use the annual growing season integrals instead of the deviation integrals to include the year 2017 in the statistical comparison.

3. Results

3.1. Drought response patterns derived from correlation analysis

3.1.1. Comparison of the correlation coefficients of vegetation indices

The correlation coefficients of the street trees studied show a wide range, from −0.85 to 0.92 (Fig. 3). We provide a more detailed figure distinguished by tree species in Appendix 2.1. For all vegetation indices, most correlations are positive, indicating that drier conditions are mostly associated with lower vegetation indices. The differences between vegetation indices are small compared to the high variance within each vegetation index correlations. However, it is noteworthy that the vegetation indices with the 20 m resolution band in the near infrared (i.e., EVI-20, NDVI-20 and NBR-20) show higher correlation coefficients than their counterparts with the 10 m resolution band (i.e., EVI-10, NDVI-10 and NBR-10). The highest correlation coefficients occur for the correlation between NBR-20 and SPEI, where 76% of the trees have positive correlation coefficients. Therefore, we select NBR-20 for the following analysis steps.

3.1.2. Species-specific cumulative drought response

Differentiating between tree species and SPEI periods in Fig. 4 reveals more distinct patterns and provides insight into the wide range observed in Fig. 3. This is because *P. x acerifolia*, which has the largest sample size, has significantly lower correlation coefficients than the other tree species. The median values of the correlation coefficients for *P. x acerifolia* are close to zero for SPEI periods of three to nine months. In contrast, those for the other species range between 0.39 and 0.63, with *Q. robur* reaching the highest median values. *P. x acerifolia* also stands out for its different relationship with the SPEI periods, which is reflected in higher correlation coefficients with SPEI-1, SPEI-12 and SPEI-24. All other tree species correlate more with SPEI periods of three to nine months. *T. cordata* shows a higher dispersion of correlation coefficients than the other species. The distributions of the correlation coefficients change when a time lag is introduced between the drought, represented by the SPEI, and the response, represented by the vegetation indices, as can be seen in Appendix 2.2.

The pairwise Wilcoxon test proves the significance of the visual

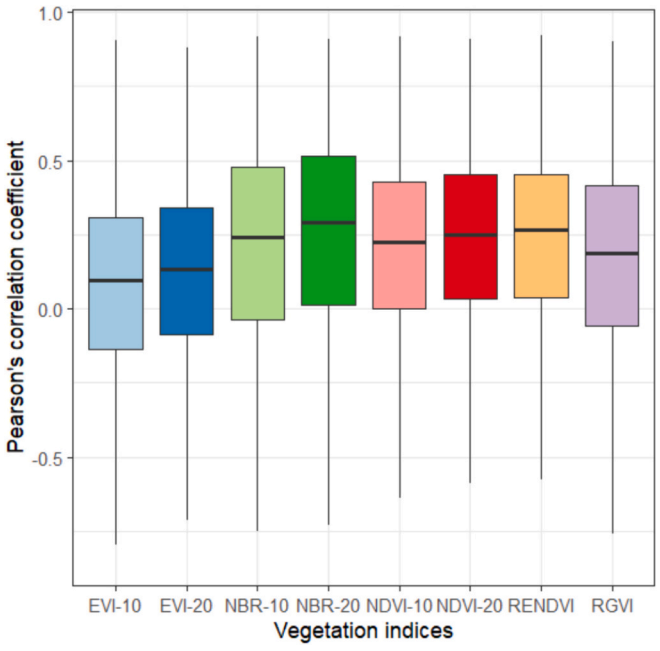

Fig. 3. Correlation of all examined trees between eight monthly median vegetation indices (for abbreviations see Table 2) and all standardised precipitation evapotranspiration indices.

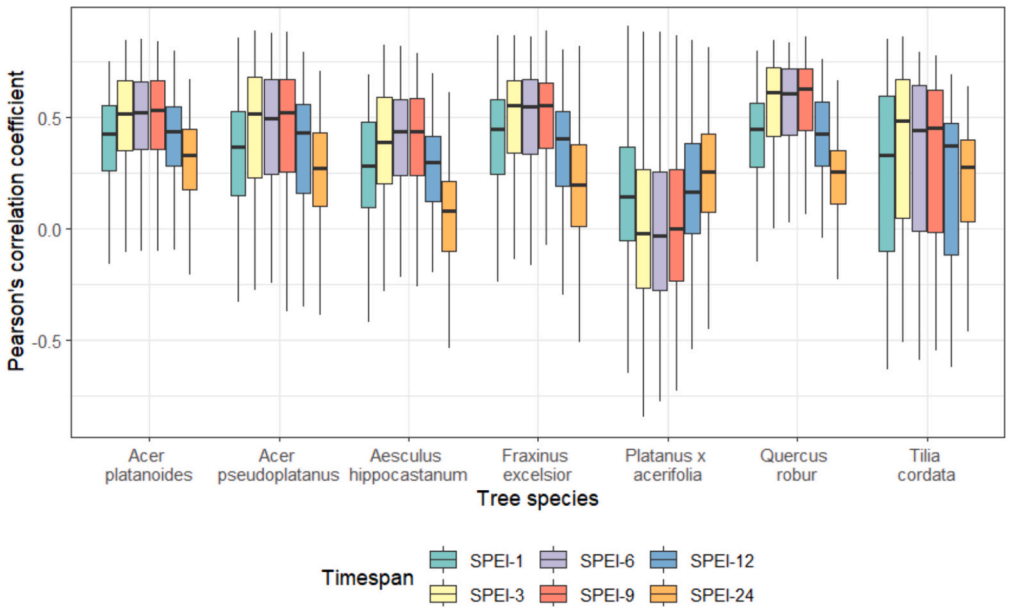

Fig. 4. Correlation between the monthly median normalised burn ratio using the 20 m resolution band and the standardised precipitation evapotranspiration index (SPEI) by tree species and SPEI period. SPEI-1, SPEI-3, SPEI-6, SPEI-9, SPEI-12, and SPEI-24 are based on accumulation periods of 1, 3, 6, 9, 12, and 24 months, respectively.

comparison between the tree species (Table 3). The median correlation coefficients for *Q. robur* and *P. x acerifolia* with the variables SPEI-6 and NBR-20 are significantly different from all other tree species at the 0.01 significance level. In addition, the median correlation coefficient for *A. hippocastanum* is significantly lower than for *F. excelsior* and *A. platanoides* at the 0.01 and 0.05 significance levels, respectively. Appendix 2.3 gives an overview of the most frequent significant positive correlations between the SPEI and the vegetation indices, considering all accumulation periods and all indices.

3.2. Drought response patterns derived from land surface phenology analysis

3.2.1. Species-specific inter- and intra-annual drought response

Fig. 5 shows the deviation of the annual growing season integrals from the 2017 baseline. Most tree species follow similar patterns with the highest deviations in 2018, followed by the years 2020, 2019, 2022, and 2021. However, there are exceptions as well as differences in the magnitude of the deviation. *T. cordata* shows a high dispersion, especially in the years 2018 and 2019. In addition, its deviation integrals are the highest compared to other species. In all years, the productivity of *T. cordata* is on average lower than in 2017. Also exceptional is the trend of *P. x acerifolia,* which shows the lowest deviations from 2017 among the tree species. In particular, the deviations in the years 2020 and 2022 are negative, which means that productivity was higher in these years than in 2017. Finally, *Q. robur* stands out for its strong differences between years.

Pairwise Wilcoxon tests on the differences in the median growing season integrals of each year confirm that the differences between the non-drought years 2017 and 2021 and the drought years 2018 and 2020 are significant at the 0.05 level for most tree species (Table 4). For five tree species, the median integrals of 2018 and 2022 are also significantly different. Notably, there are no significant differences in the median integrals between any of the years for *T. cordata*.

3.2.2. Temporal patterns of single tree drought response

Not all trees of a species respond equally to drought, as can be seen from the high dispersion in Fig. 4 and Fig. 5. In fact, trees that show a high deviation integral in 2018 are often the same trees that respond most strongly to drought in the other drought years, i.e., 2019, 2020, and 2022 (Fig. 6). Trees that are not affected by drought in 2018 show a weaker drought response in these years. Deviation integrals in the non-drought year 2021 reveal an ambivalent picture, with trees that are severely affected in 2018 showing mixed signs of recovery. Species-specific findings include *T. cordata*, which is characterised by high dispersion, especially in the years 2018 and 2019. *Q. robur* trees behave very similarly to each other with marked differences between the years. *P. x acerifolia* has on average the smallest deviation integrals compared to 2017, but some trees fall out of the pattern with very high deviations of up to 62, indicating methodological limitations (Section 4.2.1). As an example, Fig. 7 shows the NBR-20 time series of a *P. x acerifolia* tree affected by this effect. From 2018 to 2019, there is a noticeable decrease

Table 3
Significance level of pairwise Wilcoxon tests between species-specific correlation coefficients between the NBR-20 and the SPEI-6.

	Acer platanoides	*Acer pseudoplatanus*	*Aesculus hippocastanum*	*Fraxinus excelsior*	*Platanus x acerifolia*	*Quercus robur*
Acer pseudoplatanus	–					
Aesculus hippocastanum	*	–				
Fraxinus excelsior	–	–	**			
Platanus x acerifolia	**	**	**	**		
Quercus robur	**	**	**	**	**	
Tilia cordata	–	–	–	*	**	**

– no significant difference in median values.
* difference in median correlation coefficients at a significance level of 0.05.
** difference in median correlation coefficients at a significance level of 0.01.

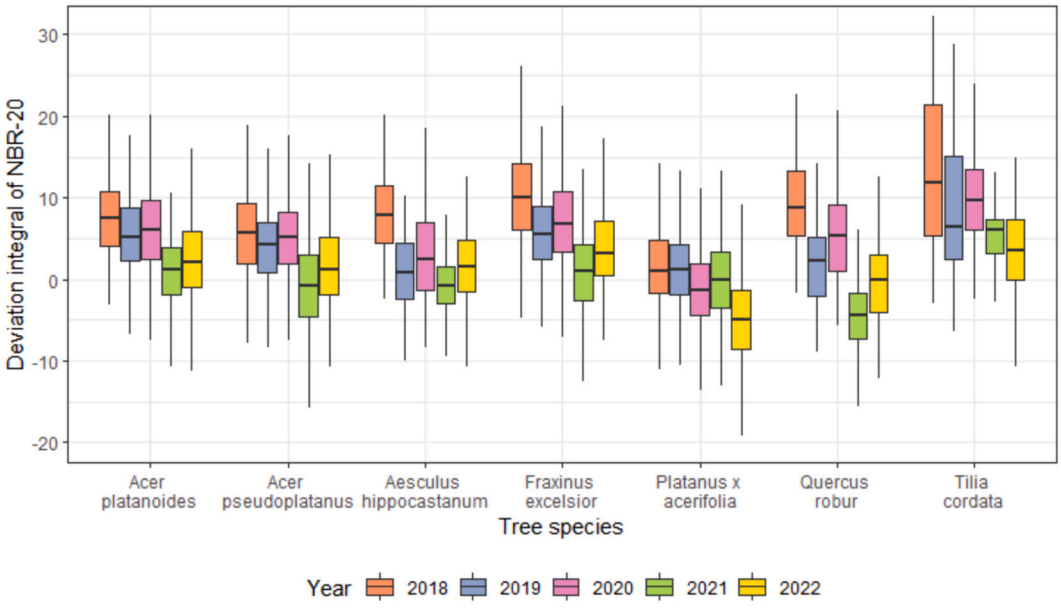

Fig. 5. Deviation integrals of the normalised burn ratio using the 20 m resolution band (NBR-20) by tree species and year.

Table 4
Significance of pairwise Wilcoxon tests between annual growing season integrals by species.

	2017	2018	2019	2020	2021
2018	* * * * *				
2019	* *	* *			
2020	* * * *	* *	*		
2021		* * * * *	* * *	* * * *	
2022	*	* * * * *	*	* *	*

Difference in median integrals at a significance level of 0.05 for …
* … *Acer platanoides*
* … *Acer pseudoplatanus*
* … *Aesculus hippocastanum*
* … *Fraxinus excelsior*
* … *Platanus x acerifolia*
* … *Quercus robur*
* … *Tilia cordata*

in the NBR-20 time series caused by construction, as inferred from aerial photos from 2017 and 2021 (Appendix 2.4). Similar effects also occur in other tree species, e.g., *A. hippocastanum*, *A. pseudoplatanus*, and *A. platanoides*, but not to such an extent.

4. Discussion

4.1. Drought response of street trees in Leipzig from 2017 to 2022

The correlation analysis reveals significant positive relationships between meteorological drought and street tree health, with drier conditions associated with lower vegetation indices (Fig. 4). This is consistent with the findings of Pluntke et al. (2021), who suggest that SPEI can explain 25 to 75% of the variability in remotely sensed vegetation indices. The land surface phenology analysis shows significant differences in tree health between drought and non-drought years (Table 4). In particular, the growing season integrals in 2017 and 2021 are significantly higher than those in 2018 and 2020 for most tree species, as expected. The drought responses in 2019 and 2022 are less pronounced. Furthermore, the deviation integrals suggest that the same trees are repeatedly affected by drought in different drought years (Fig. 6). Apart from these general findings, most drought responses vary between and within tree species, as already shown by Miller et al. (2020).

4.1.1. Variability of drought response across tree species

The results show that the tree species respond to drought at different times and to different degrees. This species-specific response is caused by different drought response strategies, such as transpiration regulation or reduced leaf area (Brune, 2016). Both drought response metrics identify *P. x acerifolia* as the species with the weakest drought response, which is consistent with previous research (Table 1). The field study by Haase and Hellwig (2022) confirms the high drought resistance of the genus *Platanus* in the city of Leipzig. According to Gillner et al. (2015), the high adaptation of *P. x acerifolia* to dry conditions is rooted in the relatively high water use efficiency. Furthermore, our observation that *P. x acerifolia* shows the highest correlations with SPEI-24 confirms the findings of Hirsch et al. (2023) and Gillner et al. (2014), who find a high sensitivity of *P. x acerifolia* to precipitation in the previous summer. All other tree species show stronger correlations using SPEI-3, SPEI-6, and

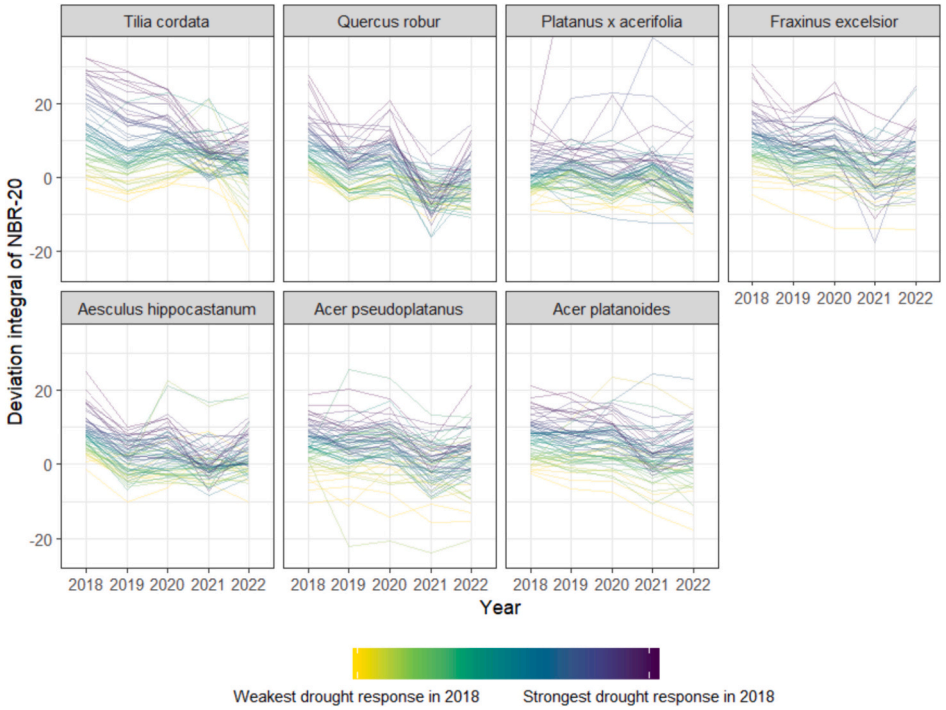

Fig. 6. Deviation integrals 2018–2022 of the normalised burn ratio using the 20 m resolution band (NBR-20) per tree. The plots show the 50 trees with the largest fractional tree cover per pixel for each tree species, coloured by the intensity of drought response in 2018, from least affected in yellow to most affected in purple. For presentation purposes, the line of a *P. x acerifolia* tree reaching a deviation integral of 62.4 in 2020 is truncated.

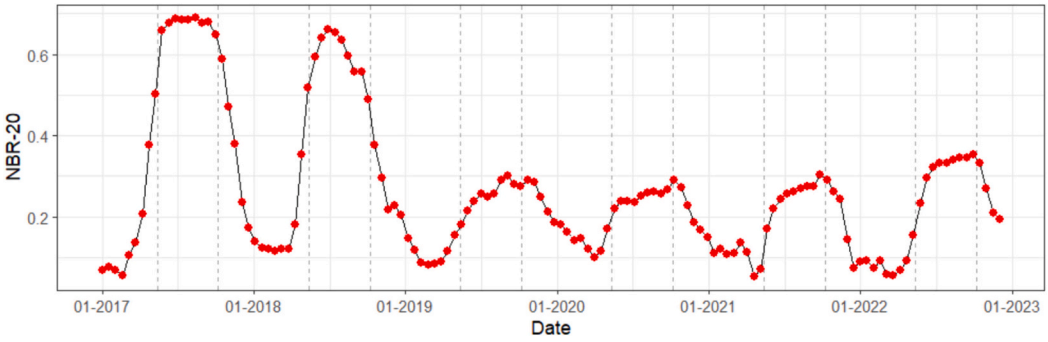

Fig. 7. Interpolated time series of the normalised burn ratio using the 20 m resolution band (NBR-20) of a *P. x acerifolia* tree, impacted by tree felling and new building construction in the surroundings. The red dots represent the 16-day interpolation, the black line the daily linear interpolation and the grey dashed lines the start and end of the growing season. (For interpretation of the references to colour in this figure legend, the reader is referred to the web version of this article.)

SPEI-9, indicating short-term drought responses. Miller et al. (2022) find that urban broadleaf forests in general show significant responses to water deficits lasting 3 to 36 months.

Q. robur differs significantly from all other species by exhibiting the strongest drought response (Table 3). Previous studies differ with regard to the drought tolerance of *Q. robur* (Table 1). On average, *Q. robur* has a medium drought tolerance. Its deep root system allows it to reach water sources during droughts (Haase and Hellwig, 2022) and it adopts an isohydric, i.e. water-saving, strategy by closing the stomata (Thomsen et al., 2020). However, stomatal closure not only reduces water loss, but also carbon fixation by photosynthesis in the short term (Jiao et al., 2021; Thomsen et al., 2020). The reduced primary production, in turn, is reflected in lower vegetation indices and could thus explain the high correlation between drought and vegetation indices of *Q. robur*. Another aspect supporting this explanation is the negative deviation integral of *Q. robur* in 2021, indicating healthier trees in 2021 than in 2017 (Fig. 5). Thus, while *Q. robur* is most sensitive to drought in the short term, it also appears to recover most effectively from prolonged drought in 2021.

The tree species *A. platanoides*, *A. pseudoplatanus*, *A. hippocastanum*, and *F. excelsior* show an intermediate drought response. This differs from previous findings where *A. pseudoplatanus* and *A. hippocastanum* are found to be the least tolerant tree species (Table 1). The discrepancy may be due to a variety of causes, such as biotic and abiotic factors other than drought, as discussed in Section 4.2.

4.1.2. Variability of drought response within tree species

In terms of within-species drought response, *T. cordata* stands out due to its highly dispersed correlation coefficients and deviation integrals in 2018 and 2019 (Fig. 4 and Fig. 5). Gillner et al. (2017) and Haase and Hellwig (2022) describe *T. cordata* as a highly adapted tree species to urban sites, preventing early leaf senescence or leaf fall even under drought conditions. In contrast, the experimental study by Stratópoulos et al. (2019) indicates premature leaf senescence of *T. cordata* and lower drought tolerance than other tree species studied, including *A. platanoides*. These contrasting results highlight the still limited research on the response of street tree to drought, which is

mostly based on experiments or field observations and therefore highly site-specific (Stratópoulos et al., 2019). Moser et al. (2017) confirm the dependence on site characteristics such as soil and microclimatic differences by comparing the water stress response of *T. cordata* trees at two different sites. Spatial clustering of the drought responses of *T. cordata* is also present in this study, as consistently indicated by both drought response metrics (Appendix 2.5). Thus, site-specific characteristics contribute to highly variable drought responses within species.

4.2. Limitations and uncertainties of drought response analysis

4.2.1. Validity of vegetation indices as indicators of vegetation health

This study has some methodological uncertainties and limitations. One limitation is the inability of vegetation indices to detect certain drought responses of trees. While changes in aboveground biomass and photosynthetic activity can be assessed with remote sensing imagery, belowground biomass dynamics, such as fine root dieback, reduced radial growth, and damages in the trunk in response to drought cannot be assessed (Schnabel et al., 2022).

Moreover, a change in vegetation index values does not necessarily indicate a drought response, but may be due to several non-drought causes, such as disease, nitrogen stress, pollution, and poor tree management (Miller et al., 2020; Wellmann, 2023; Zeng et al., 2020). Vegetation indices are not able to distinguish between these different causes of vegetation damage (Chuvieco, 2020).

In addition to the various causes of tree stress, land cover and land use around street trees affect the vegetation index time series (Helman, 2018). This is evident in Fig. 6, where trees of the species *P. x acerifolia* and *A. hippocastanum* show comparatively high deviation integrals due to land cover changes caused by tree felling and construction. Conversely, an *A. pseudoplatanus* tree has a negative deviation integral of less than −20 because young trees have been planted and irrigated in the surrounding area (Stadt Leipzig, 2023). We expect that the correlation between the vegetation indices and the SPEI would be stronger if the pixels affected by land use or land cover change were excluded. In future studies, we propose to do this by analysing land cover changes in the pixels surrounding the trees, such as surface sealing, construction or desealing. In addition to land use and land cover change, the vegetation surrounding trees might respond differently to drought, thereby affecting vegetation indices. For example, grasses are more sensitive to water shortages than trees (Allen et al., 2021). We assume such an effect for a number of *T. cordata* trees bordering agricultural land (Appendix 2.5).

Previous research disagrees on which vegetation index best describes drought responses. For example, Fang et al. (2020) find the NDVI to be the most sensitive in determining tree health conditions. In contrast, Löw and Koukal (2020) find RGVI to be the best vegetation index due to its robustness to outliers. Fang et al. (2020) suggest that the suitability of vegetation indices may depend on the studied tree species being analysed. In this study, however, the correlation coefficients of eight vegetation indices are consistent in identifying *P. x acerifolia* as the least drought-affected and *Q. robur* as the most drought-affected tree species, as well as in showing the highest dispersion for *T. cordata* (Appendix 2.1). This observation is consistent with previous research by Miller et al. (2020), which indicates that vegetation responses to drought are consistently manifested in both water- and greenness related vegetation indices. Thus, although vegetation indices describe different vegetation traits, they produce similar results.

Other candidate indices for monitoring drought effects are the leaf area index (LAI) or the fraction of absorbed photosynthetically active radiation (fAPAR). For example, Liu et al. (2021) use the LAI to analyse the drought response of tropical forests, Miraglio et al. (2020) use it to monitor vegetation health in woodland savannas and Ma et al. (2023) use it together with the fAPAR to study forest drought stress in China. These indices could be promising additional drought monitoring tools as they relate more directly to biophysical changes in the canopy. However, to our knowledge, they have not been used in an urban setting, where uncertainties could be high due to the strong background signal (Mulla, 2013; Tao et al., 2016). Given the wide range of indices already used in our study, this is beyond the scope of this study, but should be investigated in future studies.

Our results suggest that the sensitivity of the narrow near-infrared band at the original 20 m resolution to drought response is consistently higher than that of the broad near-infrared band at the 10 m resolution (Fig. 3). This is consistent with previous findings that the narrow near-infrared band is important for tree species classification (Bolyn et al., 2018; Persson et al., 2018). The higher correlation of the 20 m band might also be related to a higher proportion of surrounding vegetation such as grass, which has a higher correlation with SPEI than trees (Li et al., 2015). Therefore, the results are less indicative of the drought response of individual trees than of groups of trees. As street trees of the same age and species are often located next to each other and their surroundings are usually paved, this may be acceptable (Fang et al., 2020).

4.2.2. Validity of correlation coefficients and land surface phenology parameters as indicators for drought response

The studied street trees are sampled in such a way that the spectral signal of a tree within a pixel is maximised. This sampling approach results in an uneven distribution of tree species and is not fully representative of the species in Leipzig. Furthermore, the sample does not include dead trees as they are not listed in the street tree cadastre. This limits the generalisability of the findings on species-specific drought tolerance and prevents conclusions on tree mortality due to drought. Despite this limitation, the sample is suitable for evaluating the introduced drought response metrics, as discussed below.

The meteorological drought indicator SPEI is based on precipitation and temperature data and allows to account for short- as well as long-term meteorological droughts (Mazza et al., 2021). However, the timing and intensity of droughts vary from place to place, for example due to differences in soil and groundwater stocks (Bernhofer et al., 2015; Schwarz et al., 2020). Schwarz et al. (2020) therefore suggest using the soil moisture index (SMI) provided by the Drought Monitor Germany (Zink et al., 2016). The disadvantage, however, is that these data do not allow a comparison of cumulative effects on different tree species.

Since smoothing and interpolation techniques have a significant impact on land surface phenology parameters, it would be valuable to create a 1-day interpolation time step and to compare different smoothing and interpolation techniques (Granero-Belinchon et al., 2020; Helman, 2018). In this study, we use radial basis function convolution filters implemented in FORCE, which offer benefits due to their adaptable kernel width depending on the data availability (Scheffler and Frantz, 2022; Schwieder et al., 2016). We suggest to compare them with Savitzky-Golay filters, following the recommendations of Granero-Belinchon et al. (2020) and Li et al. (2017) for urban areas.

The growing season integral also has certain limitations. While the fixed start and end dates of the growing season are useful for year-to-year comparisons, this approach lacks the flexibility to account for annual shifts in the growing seasons. To overcome this limitation, we propose to use growing season periods of the same length but with flexible start and end dates, allowing yearly comparisons and accounting for potential shifts in the growing season.

Following Miller et al. (2020), we overcome the differences in fractional tree cover by relating the indicators to a baseline. We choose the year 2017 as the baseline because it is hardly affected by drought. The reliability of the results could be improved by using an ensemble of years as the baseline to reduce the effects of phenological characteristics of one year. Moreover, the short time series availability means that long-term trends cannot be separated from the disturbance analysis. For example, an acceleration of tree growth due to climate change could cause the small deviation integrals in 2019 and 2022 (Pretzsch et al.,

2017). These issues will be resolved when longer Sentinel-2 time series become available.

Lastly, there is uncertainty due to the lack of ground truthing data. Despite the consistency between the two drought response metrics, they still need to be verified against the drought response of street trees observed from the ground. However, collecting such data is beyond the scope of this study. To address this limitation, we use statistical tests to compare the annual and species-specific drought responses with existing literature. Other studies overcome this problem with higher-resolution time series data, such as those collected by drones (Nill et al., 2022).

4.3. Applicability of Sentinel-2 time series for street tree monitoring

4.3.1. Satellite-derived drought response of street trees as basis for urban green management

Reductions in tree health can impact their ecosystem service provision. Borgogno-Mondino and Fissore (2022) suggest a positive relationship between annual growing season integrals and ecosystem services provided by vegetation. Allen et al. (2021) support this assumption by demonstrating reduced cooling by drought-affected urban trees. The heat mitigation mechanism of urban trees through shading and evapotranspiration is limited when trees experience early leaf senescence, reduced photosynthesis, and, consequently, a lower leaf mass (Stratópoulos et al., 2019). This example of reduced heat mitigation illustrates the importance of maintaining healthy trees for their ecosystem services, and therefore, the importance of effective urban green management.

Such effective management requires information on the current state of tree health and the location of damaged trees (Borgogno-Mondino and Fissore, 2022). This spatial and temporal tree monitoring can be provided by remote sensing time series analysis, as demonstrated in this study. We see particular potential in the use of deviation integrals for urban green management. Unlike correlation coefficients, deviation integrals not only locate drought-affected trees, but also provide information on the timing of drought-induced damages. They can also be used to identify trees that are repeatedly more vulnerable to drought. For example, the participatory citizens' project "*Leipzig gießt*" (Leipzig waters), which informs about the water needs of urban trees and motivates citizens to water, could benefit from the information provided by the drought response metrics (Stadt Leipzig, 2023).

However, this capability does not make remote sensing time series a one-size-fits-all solution. Urban green management needs to consider conditions and processes at different spatial scales, from global climate change to local use patterns, as well as linkages between social and ecological systems, such as the heat vulnerability of residents and equitable access to green spaces for all residents (Wellmann, 2023). This also means considering the trade-offs between ecosystem services and disservices, such as infrastructure damage (Salmond et al., 2016). In Leipzig, for example, older residents value landscape aesthetics, while younger residents prioritize sports facilities, and all age groups consider litter in green spaces to be a major disservice (Palliwoda and Priess, 2021). Thus, remote sensing should be embedded in a holistic approach that includes, for example, field measurements and surveys with residents to provide a profound basis for decision-making (Salmond et al., 2016; Wellmann, 2023).

Various urban green management measures could benefit from such holistic approaches that incorporate remote sensing. For example, based on solely this study, one might propose to plant new *P. x acerifolia* trees. While this is a good choice in terms of their high drought tolerance, it neglects other needed tree traits and values, such as supporting ecosystem services for biodiversity. Gloor and Hofbauer (2018), for example, rate *P. x acerifolia* as the worst of the tree species studied in terms of biodiversity value. These contrary arguments represent only two of many criteria for new tree plantings, such as tolerance to other biotic or abiotic stressors, such as diseases or frost, urban land-use conflicts, and aesthetic considerations (Brune, 2016; Mullaney et al., 2015). The example demonstrates that there is no general solution for urban green management, but that holistic solutions are needed, to which remote sensing can contribute.

4.3.2. Satellite-derived drought response of street trees as basis for further research

Despite the limited generalizability of this study, the developed workflow is promising for further urban ecological research as sample sizes increase. Remote sensing time series prove to be suitable for effective monitoring of vegetation drought response at a high spatial and temporal resolution and, with continuous acquisitions, also for long-term monitoring, thereby overcoming the limitations of traditional field observations.

As remote sensing time series only capture some drought-related tree damage, they could benefit from the integration of other data, such as from dendrochronological research and field observations provided by citizen science projects. These can be complementary, as dendrochronological analysis does not indicate changes in the canopy, while remote sensing cannot measure radial growth (Schnabel et al., 2022). One promising way to collect field data on tree damage is through citizen science projects. This could enable the collection of spatially and temporally highly resolved data, involve citizens in ecological research, and integrate their local knowledge (Kobori et al., 2016). Thus, green management and research on drought responses of trees would profit from mixed-method approaches.

Another application of drought response metrics is research into the causes and consequences of drought-induced damage. Factors affecting vegetation health include irrigation systems, LST, distance to lakes, and distance to roads (Cârlan et al., 2020). Analysing the relationship between multiple drivers and drought response could enable predictions under climate change and urbanisation scenarios including mortality, potential tipping points, and recovery. The feedback of drought-damaged street trees to their urban surroundings in terms of their cooling potential and other ecosystem service provision remains understudied (Jochner and Menzel, 2015). Thus, drought response metrics, in combination with other approaches, have a high potential for application in future scientific research on the determinants and consequences of drought response.

5. Conclusion

The city of Leipzig experienced prolonged periods of severe drought from 2018 to 2022. Maintaining the health of street trees, and thus the provision of ecosystem services, under such drought conditions is a major challenge for many urban areas worldwide and is becoming increasingly important under climate change. This study explores the potential of remote sensing to provide information on temporal and species-specific drought response patterns by developing and evaluating two drought response metrics derived from Sentinel-2 vegetation index time series. While one metric is built on the correlation between multiple vegetation indices and meteorological drought conditions represented by SPEI, the second metric uses deviations of annual growing season integrals of vegetation index time series from the 2017 baseline.

The correlation analysis reveals that the NBR-20 relates strongest to the meteorological drought indicator. Both drought response metrics are consistent with the drought related traits of the different tree species, e.g., by identifying *P. x acerifolia* as the most drought resistant tree species. The other tree species show positive correlation coefficients for drought periods of three to nine months, indicating a response to drought within the same year of dry conditions. This observation is also reflected in the growing season integrals, which are significantly lower for most species in the drought years 2018 and 2020 than in the non-drought year 2017. Both drought response metrics capture most species-specific and temporal patterns and can be considered complementary. Correlation coefficients excel at capturing the different temporal characteristics of droughts by describing their cumulative effects on street trees, while

deviation integrals offer an advantage in distinguishing drought response strengths across years, thereby allowing the analysis of the persistence of drought-induced damage.

Future work needs to deepen the validation of the drought response metrics with field observations, such as dendrochronological studies. Further, both metrics would benefit from being embedded in mixed-method approaches to more fully incorporate multiple perspectives, such as biodiversity and drought resilience. In the context of climate change, where today's extreme conditions are becoming tomorrow's new normal, holistic approaches and solutions to urban greenery are becoming increasingly important.

AI statement

During the preparation of this work the author(s) used ChatGPT to improve the phrasing, spelling and grammar of the manuscript as well as to search for solutions to errors expressed by R. After using this tool, the author(s) reviewed and edited the content as needed and take(s) full responsibility for the content of the publication.

Funding

This research was supported by the project BiNatUr: Bringing nature back – biodiversity-friendly nature-based solutions in cities and funded through the 2020–2021 Biodiversa and Water JPI joint call for research projects, under the BiodivRestore ERA-NET Cofund (GA N°101003777), with the EU and the funding organisations Academy of Finland (Finland), Bundesministerium für Bildung und Forschung (BMBF, Germany), Federal Ministry of Education and Research (Germany), National Science Centre (Poland), Research Foundation Flanders (fwo, Belgium) and Fundação para a Ciência e Tecnologia (Portugal). We acknowledge support by the Open Access Publication Fund of Humboldt-Universität zu Berlin.

CRediT authorship contribution statement

Leonie Leisenheimer: Writing – original draft, Visualization, Validation, Software, Methodology, Formal analysis, Conceptualization. **Thilo Wellmann:** Writing – review & editing, Supervision, Conceptualization. **Clemens Jänicke:** Writing – review & editing, Investigation, Data curation. **Dagmar Haase:** Writing – review & editing, Supervision, Conceptualization.

Declaration of competing interest

The authors declare that they have no known competing financial interests or personal relationships that could have appeared to influence the work reported in this paper.

Data availability

The data and scripts developed as part of this study can be accessed via Zenodo at https://doi.org/10.5281/zenodo.11550407

Appendix A. Supplementary data

Supplementary information to this article can be found online at https://doi.org/10.1016/j.ecoinf.2024.102659.

References

Allen, M.A., Roberts, D.A., McFadden, J.P., 2021. Reduced urban green cover and daytime cooling capacity during the 2012–2016 California drought. Urban Clim. 36, 100768 https://doi.org/10.1016/j.uclim.2020.100768.

Aryal, J., Sitaula, C., Aryal, S., 2022. NDVI threshold-based urban green space mapping from sentinel-2A at the local governmental area (LGA) level of Victoria, Australia. Land 11 (3), 351. https://doi.org/10.3390/land11030351.

Beguería, S., Vicente-Serrano, S.M., 2023. Package 'SPEI' [computer software]. https://cran.r-project.org/web/packages/SPEI/SPEI.pdf.

Bernhofer, C., Hänsel, S., Schaller, A., Pluntke, T., 2015. Charakterisierung meteorologischer Trockenheit. Schriftenreihe LfULG 7, 1–208. https://publikationen.sachsen.de/bdb/artikel/24200 (Accessed 2023-04-11).

Bolyn, C., Michez, A., Gaucher, P., Lejeune, P., Bonnet, S., 2018. Forest mapping and species composition using supervised per pixel classification of Sentinel-2 imagery. BASE 22 (3), 172–187. https://doi.org/10.25518/1780-4507.16524.

Borgogno-Mondino, E., Fissore, V., 2022. Reading greenness in urban areas: possible roles of phenological metrics from the Copernicus HR-VPP dataset. Remote Sens. 14 (18), 4517. https://doi.org/10.3390/rs14184517.

Brooks, B.-G.J., Lee, D.C., Pomara, L.Y., Hargrove, W.W., 2020. Monitoring broadscale vegetational diversity and change across north American landscapes using land surface phenology. Forests 11 (6), 606. https://doi.org/10.3390/f11060606.

Brune, M., 2016. Urban trees under climate change. Potential impacts of dry spells and heat waves in three German regions in the 2050s. Clim. Serv. Center Germany 1–123. Report 24. https://epub.sub.uni-hamburg.de/epub/volltexte/2017/69269/pdf/report_24.pdf (Accessed 2023-04-12).

Caparros-Santiago, J.A., Rodriguez-Galiano, V., Dash, J., 2021. Land surface phenology as indicator of global terrestrial ecosystem dynamics: A systematic review. ISPRS J. Photogramm. Remote Sens. 171, 330–347. https://doi.org/10.1016/j.isprsjprs.2020.11.019.

Cârlan, I., Mihai, B.-A., Nistor, C., Große-Stoltenberg, A., 2020. Identifying urban vegetation stress factors based on open access remote sensing imagery and field observations. Eco. Inform. 55, 101032 https://doi.org/10.1016/j.ecoinf.2019.101032.

Chuvieco, E., 2020. Fundamentals of Satellite Remote Sensing: An Environmental Approach, Third edition. CRC Press Taylor & Francis Group.

Ciesielski, M., Sterenczak, K., 2019. Accuracy of determining specific parameters of the urban forest using remote sensing. IForest 12 (6), 498–510. https://doi.org/10.3832/ifor3024-012.

Crawley, M.J., 2013. The R Book, Second edition. Wiley. https://doi.org/10.1002/9781118448908.

Deutscher Wetterdienst [DWD], 2023. Climate Data Center. https://opendata.dwd.de/climate_environment/CDC/ (Accessed 2023-04-18).

Duarte, L., Teodoro, A.C., Gonçalves, H., 2014. Deriving phenological metrics from NDVI through an open source tool developed in QGIS. In: SPIE Proceedings, Earth Resources and Environmental Remote Sensing/GIS Applications V. SPIE, p. 924511. https://doi.org/10.1117/12.2066136.

European Space Agency [ESA], 2023. Sentinel-2: About the launch. https://www.esa.int/Applications/Observing_the_Earth/Copernicus/Sentinel-2/About_the_launch (Accessed 2023-04-18).

Fang, F., McNeil, B., Warner, T., Dahle, G., Eutsler, E., 2020. Street tree health from space? An evaluation using WorldView-3 data and the Washington D.C. street tree spatial database. Urban For. Urban Green. 49, 126634 https://doi.org/10.1016/j.ufug.2020.126634.

Frantz, D., 2019. FORCE – Landsat + Sentinel-2 analysis ready data and beyond. Remote Sens. 11 (9), 1124. https://doi.org/10.3390/rs11091124.

Frantz, D., Stellmes, M., Roder, A., Udelhoven, T., Mader, S., Hill, J., 2016. Improving the spatial resolution of land surface phenology by fusing medium- and coarse-resolution inputs. IEEE Trans. Geosci. Remote Sens. 54 (7), 4153–4164. https://doi.org/10.1109/TGRS.2016.2537929.

Fuchs, T., 2022. Stärkste Grundwasserdürre seit 100 Jahren beobachtet: Klimatologische Einordnung des Jahres 2021 in Sachsen. https://www.dwd.de/DE/klimaumwelt/aktuelle_meldungen/220126/grundwasserduerre_sachsen.html.

García-Pardo, K.A., Moreno-Rangel, D., Domínguez-Amarillo, S., García-Chávez, J.R., 2022. Remote sensing for the assessment of ecosystem services provided by urban vegetation: A review of the methods applied. Urban For. Urban Green. 74, 127636 https://doi.org/10.1016/j.ufug.2022.127636.

Gessner, U., Naeimi, V., Klein, I., Kuenzer, C., Klein, D., Dech, S., 2013. The relationship between precipitation anomalies and satellite-derived vegetation activity in Central Asia. Glob. Planet. Chang. 110, 74–87. https://doi.org/10.1016/j.gloplacha.2012.09.007.

Gillner, S., Bräuning, A., Roloff, A., 2014. Dendrochronological analysis of urban trees: climatic response and impact of drought on frequently used tree species. Trees 28 (4), 1079–1093. https://doi.org/10.1007/s00468-014-1019-9.

Gillner, S., Korn, S., Roloff, A., 2015. Leaf-gas exchange of five tree species at urban street sites. Arboricult. Urban For. 41 (3), 113–124. https://doi.org/10.48044/jauf.2015.012.

Gillner, S., Korn, S., Hofmann, M., Roloff, A., 2017. Contrasting strategies for tree species to cope with heat and dry conditions at urban sites. Urban Ecosyst. 20 (4), 853–865. https://doi.org/10.1007/s11252-016-0636-z.

Gitelson, A., Merzlyak, M.N., 1994. Spectral reflectance changes associated with autumn senescence of Aesculus hippocastanum L. and Acer platanoides L. leaves: spectral features and relation to chlorophyll estimation. J. Plant Physiol. 143 (3), 286–292. https://doi.org/10.1016/S0176-1617(11)81633-0.

Gloor, S., Hofbauer, M.G., 2018. Der ökologische Wert von Stadtbäumen bezüglich der Biodiversität. In: Dujesiefken, D. (Ed.), Jahrbuch der Baumpflege 2018: Yearbook of Arboriculture, vol. 22. Haymarket Media, pp. 33–48.

Granero-Belinchon, C., Adeline, K., Lemonsu, A., Briottet, X., 2020. Phenological dynamics characterization of alignment trees with Sentinel-2 imagery: A vegetation indices time series reconstruction methodology adapted to urban areas. Remote Sens. 12 (4), 639. https://doi.org/10.3390/rs12040639.

Guzmán, Q.J.A., Pinto-Ledezma, J.N., Frantz, D., Townsend, P.A., Juzwik, J., Cavender-Bares, J., 2023. Mapping oak wilt disease using phenological observations from space. https://doi.org/10.1101/2023.05.25.542318.

Haase, D., Hellwig, R., 2022. Effects of heat and drought stress on the health status of six urban street tree species in Leipzig, Germany. Trees Forests People 8, 100252. https://doi.org/10.1016/j.tfp.2022.100252.
Haase, D., Jänicke, C., Wellmann, T., 2019. Front and back yard green analysis with subpixel vegetation fractions from earth observation data in a city. Landsc. Urban Plan. 182, 44–54. https://doi.org/10.1016/j.landurbplan.2018.10.010.
Helman, D., 2018. Land surface phenology: what do we really 'see' from space? Sci. Total Environ. 618, 665–673. https://doi.org/10.1016/j.scitotenv.2017.07.237.
Hessisches Landesamt für Naturschutz, Umwelt und Geologie [HLNUG], 2023. Stadtgrün Onlinetool: Klimaresiliente Baumarten finden!. https://www.hlnug.de/themen/klimawandel-und-anpassung/projekte/klimprax-stadtgruen/online-tool/klimaresiliente-baumarten-finden (Accessed 2023-04-18).
Hirsch, M., Böddeker, H., Albrecht, A., Saha, S., 2023. Drought tolerance differs between urban tree species but is not affected by the intensity of traffic pollution. Trees 37 (1), 111–131. https://doi.org/10.1007/s00468-022-02294-0.
Huete, A., Didan, K., Miura, T., Rodriguez, E., Gao, X., Ferreira, L., 2002. Overview of the radiometric and biophysical performance of the MODIS vegetation indices. Remote Sens. Environ. 83 (1–2), 195–213. https://doi.org/10.1016/S0034-4257(02)00096-2.
Imbery, F., Friedrich, K., Fleckenstein, R., Plückhahn, B., Brömser, A., Bissolli, P., Daßler, J., Haeseler, S., Rustemeier, E., Ziese, M., Breidenbach, J.-N., Fränkling, S., Trentmann, J., Kaspar, F., 2023. Klimatologischer Rückblick auf 2022: Das sonnenscheinreichste und eines der beiden wärmsten Jahre in Deutschland. https://www.dwd.de/DE/klimaumwelt/aktuelle_meldungen/230123/download_jahresrueckblick-2022.pdf?__blob=publicationFile&v=1 (Accessed 2023-04-18).
Jain, S.K., Keshri, R., Goswami, A., Sarkar, A., 2010. Application of meteorological and vegetation indices for evaluation of drought impact: a case study for Rajasthan, India. Nat. Hazards 54 (3), 643–656. https://doi.org/10.1007/s11069-009-9493-x.
Ji, L., Peters, A.J., 2003. Assessing vegetation response to drought in the northern Great Plains using vegetation and drought indices. Remote Sens. Environ. 87 (1), 85–98. https://doi.org/10.1016/S0034-4257(03)00174-3.
Jiao, W., Wang, L., McCabe, M.F., 2021. Multi-sensor remote sensing for drought characterization: current status, opportunities and a roadmap for the future. Remote Sens. Environ. 256, 112313 https://doi.org/10.1016/j.rse.2021.112313.
Jochner, S., Menzel, A., 2015. Urban phenological studies - past, present, future. Environ. Pollut. 203, 250–261. https://doi.org/10.1016/j.envpol.2015.01.003.
Kabisch, N., Kraemer, R., Brenck, M.E., Haase, D., Lausch, A., Luttkus, M.L., Mueller, T., Remmler, P., Döhren, P., Voigtländer, J., Bumberger, J., 2021. A methodological framework for the assessment of regulating and recreational ecosystem services in urban parks under heat and drought conditions. Ecosyst. People 17 (1), 464–475. https://doi.org/10.1080/26395916.2021.1958062.
Key, C.H., Benson, N.C., 2006. Landscape assessment (LA): sampling and analysis methods. In: Lutes, D.C., Keane, R.E., Caratti, J.F., Key, C.H., Benson, N.C., Sutherland, S., Gangi, L.J. (Eds.), FIREMON: Fire Effects Monitoring and Inventory System (LA-1-55).
Kobori, H., Dickinson, J.L., Washitani, I., Sakurai, R., Amano, T., Komatsu, N., Kitamura, W., Takagawa, S., Koyama, K., Ogawara, T., Miller-Rushing, A.J., 2016. Citizen science: a new approach to advance ecology, education, and conservation. Ecol. Res. 31 (1), 1–19. https://doi.org/10.1007/s11284-015-1314-y.
Kogan, F.N., 1990. Remote sensing of weather impacts on vegetation in non-homogeneous areas. Int. J. Remote Sens. 11 (8), 1405–1419. https://doi.org/10.1080/01431169008955102.
Kopecká, M., Szatmári, D., Rosina, K., 2017. Analysis of urban green spaces based on sentinel-2A: case studies from Slovakia. Land 6 (2), 25. https://doi.org/10.3390/land6020025.
Kraemer, R., Kabisch, N., 2022. Parks under stress: air temperature regulation of urban green spaces under conditions of drought and summer heat. Front. Environ. Sci. 10, 849965 https://doi.org/10.3389/fenvs.2022.849965.
Krehbiel, C.P., Jackson, T., Henebry, G.M., 2016. Web-enabled Landsat data time series for monitoring urban heat island impacts on land surface phenology. IEEE J. Sel. Top. Appl. Earth Obs. Remote Sens. 9 (5), 2043–2050. https://doi.org/10.1109/JSTARS.2015.2496951.
Li, Z., Zhou, T., Zhao, X., Huang, K., Gao, S., Wu, H., Luo, H., 2015. Assessments of drought impacts on vegetation in China with the optimal time scales of the climatic drought index. Int. J. Environ. Res. Public Health 12 (7), 7615–7634. https://doi.org/10.3390/ijerph120707615.
Li, F., Song, G., Liujun, Z., Yanan, Z., Di, L., 2017. Urban vegetation phenology analysis using high spatio-temporal NDVI time series. Urban For. Urban Green. 25, 43–57. https://doi.org/10.1016/j.ufug.2017.05.001.
Liu, L., Gong, F., Chen, X., Su, Y., Fan, L., Wu, S., Yang, X., Zhang, J., Yuan, W., Ciais, P., Zhou, C., 2021. Bidirectional drought-related canopy dynamics across pantropical forests: A satellite-based statistical analysis. Remote Sens. Ecol. Conserv. 8 (1), 72–91. https://doi.org/10.1002/rse2.229.
Löw, M., Koukal, T., 2020. Phenology modelling and forest disturbance mapping with Sentinel-2 time series in Austria. Remote Sens. 12 (24), 4191. https://doi.org/10.3390/rs12244191.
Ma, H., Cui, T., Cao, L., 2023. Monitoring of drought stress in Chinese forests based on satellite solar-induced chlorophyll fluorescence and multi-source remote sensing indices. Remote Sens. 15 (4), 879. https://doi.org/10.3390/rs15040879.
Mazza, G., Markou, L., Sarris, D., 2021. Species-specific growth dynamics and vulnerability to drought at the single tree level in a Mediterranean reforestation. Trees 35 (5), 1697–1710. https://doi.org/10.1007/s00468-021-02151-6.
Miller, D.L., Alonzo, M., Roberts, D.A., Tague, C.L., McFadden, J.P., 2020. Drought response of urban trees and turfgrass using airborne imaging spectroscopy. Remote Sens. Environ. 240, 111646 https://doi.org/10.1016/j.rse.2020.111646.
Miller, D.L., Alonzo, M., Meerdink, S.K., Allen, M.A., Tague, C.L., Roberts, D.A., McFadden, J.P., 2022. Seasonal and interannual drought responses of vegetation in a California urbanized area measured using complementary remote sensing indices. ISPRS J. Photogramm. Remote Sens. 183, 178–195. https://doi.org/10.1016/j.isprsjprs.2021.11.002.
Miraglio, T., Adeline, K., Huesca, M., Ustin, S., Briottet, X., 2020. Monitoring LAI, chlorophylls, and carotenoids content of a woodland savanna using hyperspectral imagery and 3D radiative transfer modeling. Remote Sens. 12 (1), 28. https://doi.org/10.3390/rs12010028.
Misra, G., Buras, A., Menzel, A., 2016. Effects of different methods on the comparison between land surface and ground phenology: A methodological case study from South-Western Germany. Remote Sens. 8 (9), 753. https://doi.org/10.3390/rs8090753.
Mittag, H.-J., 2017. Statistik: Eine Einführung mit interaktiven Elementen, Fifth edition. Springer.
Moser, A., Rahman, M.A., Pretzsch, H., Pauleit, S., Rötzer, T., 2017. Inter- and intraannual growth patterns of urban small-leaved lime (Tilia cordata mill.) at two public squares with contrasting microclimatic conditions. Int. J. Biometeorol. 61 (6), 1095–1107. https://doi.org/10.1007/s00484-016-1290-0.
Motohka, T., Nasahara, K.N., Oguma, H., Tsuchida, S., 2010. Applicability of green-red vegetation index for remote sensing of vegetation phenology. Remote Sens. 2 (10), 2369–2387. https://doi.org/10.3390/rs2102369.
Mulla, D.J., 2013. Twenty five years of remote sensing in precision agriculture: Key advances and remaining knowledge gaps. Biosyst. Eng. 114 (4), 358–371. https://doi.org/10.1016/j.biosystemseng.2012.08.009.
Mullaney, J., Lucke, T., Trueman, S.J., 2015. A review of benefits and challenges in growing street trees in paved urban environments. Landsc. Urban Plan. 134, 157–166. https://doi.org/10.1016/j.landurbplan.2014.10.013.
Nagler, P., Scott, R., Westenburg, C., Cleverly, J., Glenn, E., Huete, A., 2005. Evapotranspiration on western U.S. rivers estimated using the enhanced vegetation index from MODIS and data from eddy covariance and Bowen ratio flux towers. Remote Sens. Environ. 97 (3), 337–351. https://doi.org/10.1016/j.rse.2005.05.011.
Nill, L., Grünberg, I., Ullmann, T., Gessner, M., Boike, J., Hostert, P., 2022. Arctic shrub expansion revealed by Landsat-derived multitemporal vegetation cover fractions in the Western Canadian Arctic. Remote Sens. Environ. 281, 113228 https://doi.org/10.1016/j.rse.2022.113228.
Palliwoda, J., Priess, J.A., 2021. What do people value in urban green? Linking characteristics of urban green spaces to users' perceptions of nature benefits, disturbances, and disservices. Ecol. Soc. 26 (1), 28. https://doi.org/10.5751/ES-12204-260128.
Persson, M., Lindberg, E., Reese, H., 2018. Tree species classification with multi-temporal Sentinel-2 data. Remote Sens. 10 (11), 1794. https://doi.org/10.3390/rs10111794.
Pluntke, T., Kronenberg, R., Hänsel, S., Rumpf, D., Zimmermann, F., Matschullat, J., Bernhofer, C., 2021. Erfassung und Abschätzung von Trockenheitsmerkmalen in Sachsen. Schriftenreihe LfULG 1, 1–122. https://publikationen.sachsen.de/bdb/artikel/36871 (Accessed 2023-04-11).
Pretzsch, H., Biber, P., Uhl, E., Dahlhausen, J., Schütze, G., Perkins, D., Rötzer, T., Caldentey, J., Koike, T., van Con, T., Chavanne, A., Du Toit, B., Foster, K., Lefer, B., 2017. Climate change accelerates growth of urban trees in metropolises worldwide. Sci. Rep. 7 (1), 15403. https://doi.org/10.1038/s41598-017-14831-w.
Qiu, T., Song, C., Zhang, Y., Liu, H., Vose, J.M., 2020. Urbanization and climate change jointly shift land surface phenology in the northern mid-latitude large cities. Remote Sens. Environ. 236, 111477 https://doi.org/10.1016/j.rse.2019.111477.
Rey-Gozalo, G., Barrigón Morillas, J.M., Montes González, D., Vílchez-Gómez, R., 2023. Influence of green areas on the urban sound environment. Curr. Pollut. Rep. 9 (4), 746–759. https://doi.org/10.1007/s40726-023-00284-5.
Roloff, A., Korn, S., Gillner, S., 2009. The climate-species-matrix to select tree species for urban habitats considering climate change. Urban For. Urban Green. 8 (4), 295–308. https://doi.org/10.1016/j.ufug.2009.08.002.
Rumpf, D., 2021a. Regionales Klimainformationssystem "ReKIS": Lufttemperatur Leipzig. https://rekisviewer.hydro.tu-dresden.de/fdm/files/REKISKOMMUNAL/SN/14713000/010_TEMPERATUR.pdf.
Rumpf, D., 2021b. Regionales Klimainformationssystem "ReKIS": Niederschlag Leipzig. https://rekisviewer.hydro.tu-dresden.de/fdm/files/REKISKOMMUNAL/SN/14713000/020_NIEDERSCHLAG.pdf.
Salmond, J.A., Tadaki, M., Vardoulakis, S., Arbuthnott, K., Coutts, A., Demuzere, M., Dirks, K.N., Heaviside, C., Lim, S., Macintyre, H., McInnes, R.N., Wheeler, B.W., 2016. Health and climate related ecosystem services provided by street trees in the urban environment. Environ. Health 15 (Suppl. 1), 36. https://doi.org/10.1186/s12940-016-0103-6.
Scheffler, D., Frantz, D., 2022. Improved burn severity estimation by using land surface phenology metrics and red edge information estimated from Landsat. Int. J. Appl. Earth Obs. Geoinf. 115, 103126 https://doi.org/10.1016/j.jag.2022.103126.
Schnabel, F., Purrucker, S., Schmitt, L., Engelmann, R.A., Kahl, A., Richter, R., Seele-Dilbat, C., Skiadaresis, G., Wirth, C., 2022. Cumulative growth and stress responses to the 2018-2019 drought in a European floodplain forest. Glob. Chang. Biol. 28 (5), 1870–1883. https://doi.org/10.1111/gcb.16028.
Schwarz, J., Skiadaresis, G., Kohler, M., Kunz, J., Schnabel, F., Vitali, V., Bauhus, J., 2020. Quantifying growth responses of trees to drought – a critique of commonly used resilience indices and recommendations for future studies. Curr. For. Rep. 6 (3), 185–200. https://doi.org/10.1007/s40725-020-00119-2.
Schwieder, M., Leitão, P.J., Da Cunha Bustamante, M.M., Ferreira, L.G., Rabe, A., Hostert, P., 2016. Mapping Brazilian savanna vegetation gradients with Landsat time series. Int. J. Appl. Earth Obs. Geoinf. 52, 361–370. https://doi.org/10.1016/j.jag.2016.06.019.

Shahtahmassebi, A.R., Li, C., Fan, Y., Wu, Y., Lin, Y., Gan, M., Wang, K., Malik, A., Blackburn, G.A., 2021. Remote sensing of urban green spaces: A review. Urban For. Urban Green. 57, 126946 https://doi.org/10.1016/j.ufug.2020.126946.

Stadt Leipzig, 2019a. In: Umwelt, Dezernat, Klima, Ordnung, Sport (Eds.), Trockenheit setzt Leipzigs Bäumen zu. https://www.leipzig.de/presse/medieninformationen/medieninformation?tx_ewerkpressrelease_pressrelease%5Baction%5D=show&tx_ewerkpressrelease_pressrelease%5Bcontroller%5D=PressRelease&tx_ewerkpressrelease_pressrelease%5BpressRelease%5D=11145&cHash=db7b8c11ec1889bcd04dae36a8a6eb81 (Accessed 2023-04-18).

Stadt Leipzig, 2019b. In: Stadtgrün, Amt Für, Gewässer (Eds.), Straßenbaumkonzept Leipzig 2030. https://static.leipzig.de/fileadmin/mediendatenbank/leipzig-de/Stadt/02.3_Dez3_Umwelt_Ordnung_Sport/67_Amt_fuer_Stadtgruen_und_Gewaesser/Baeume_Baumschutz/Stadtbaeume/Strassenbaumkonzept_Leipzig_2030.pdf (Accessed 2023-04-04).

Stadt Leipzig, 2020. In: Stadtgrün, Amt Für, Gewässer (Eds.), Straßenbaumkataster Leipzig. https://opendata.leipzig.de/dataset/strassenbaumkataster (Accessed 2023-04-18).

Stadt Leipzig, 2021. In: Umweltschutz, Amt Für (Ed.), Leipzig Klimaanalyse – Phase II: Erweiterung der Planungshinweiskarte. https://static.leipzig.de/fileadmin/mediendatenbank/leipzig-de/Stadt/02.3_Dez3_Umwelt_Ordnung_Sport/36_Amt_fuer_Umweltschutz/Energie_und_Klima/Stadtklima/Abschlussbericht_ohne_Karten_Stadtklimaanalyse_Phase_II_Leipzig.pdf (Accessed 2023-04-18).

Stadt Leipzig, 2023. In: Stadtgrün, Amt Für, Gewässer (Eds.), Bewässerung von Stadtbäumen. https://www.leipzig.de/umwelt-und-verkehr/umwelt-und-naturschutz/baeume-und-baumschutz/bewaesserung-von-stadtbaeumen (Accessed 2023-04-18).

Stratópoulos, L.M.F., Zhang, C., Duthweiler, S., Häberle, K.-H., Rötzer, T., Xu, C., Pauleit, S., 2019. Tree species from two contrasting habitats for use in harsh urban environments respond differently to extreme drought. Int. J. Biometeorol. 63 (2), 197–208. https://doi.org/10.1007/s00484-018-1653-9.

Tao, X., Liang, S., He, T., Jin, H., 2016. Estimation of fraction of absorbed photosynthetically active radiation from multiple satellite data: model development and validation. Remote Sens. Environ. 184, 539–557. https://doi.org/10.1016/j.rse.2016.07.036.

Thomsen, S., Reisdorff, C., Gröngröft, A., Jensen, K., Eschenbach, A., 2020. Responsiveness of mature oak trees (Quercus robur L.) to soil water dynamics and meteorological constraints in urban environments. Urban Ecosyst. 23 (1), 173–186. https://doi.org/10.1007/s11252-019-00908-z.

TU Dresden, 2015. In: Forstbotanik, Professur Für (Ed.), citree: ein Forschungsprojekt der TU Dresden (2012–2015). https://citree.de/db-names.php (Accessed 2023-04-18).

Tucker, C.J., 1979. Red and photographic infrared linear combinations for monitoring vegetation. Remote Sens. Environ. 8 (2), 127–150. https://doi.org/10.1016/0034-4257(79)90013-0.

van der Linden, S., Okujeni, A., Canters, F., Degerickx, J., Heiden, U., Hostert, P., Priem, F., Somers, B., Thiel, F., 2019. Imaging spectroscopy of urban environments. Surv. Geophys. 40 (3), 471–488. https://doi.org/10.1007/s10712-018-9486-y.

Vicente-Serrano, S.M., Beguería, S., López-Moreno, J.I., 2010. A multiscalar drought index sensitive to global warming: the standardized precipitation evapotranspiration index. J. Clim. 23 (7), 1696–1718. https://doi.org/10.1175/2009JCLI2909.1.

Wellmann, T., 2023. Remote Sensing for Sustainable and Resilient Cities: New Pathways to Support Social-Ecological Systems in Change. Doctoral dissertation. Humboldt University of Berlin, Mathematisch-Naturwissenschaftliche Fakultät. https://doi.org/10.18452/26450.

Wellmann, T., Lausch, A., Andersson, E., Knapp, S., Cortinovis, C., Jache, J., Scheuer, S., Kremer, P., Mascarenhas, A., Kraemer, R., Haase, A., Schug, F., Haase, D., 2020. Remote sensing in urban planning: contributions towards ecologically sound policies? Landsc. Urban Plan. 204, 103921 https://doi.org/10.1016/j.landurbplan.2020.103921.

Zeng, L., Wardlow, B.D., Xiang, D., Hu, S., Li, D., 2020. A review of vegetation phenological metrics extraction using time-series, multispectral satellite data. Remote Sens. Environ. 237, 111511 https://doi.org/10.1016/j.rse.2019.111511.

Zhao, A., Yu, Q., Feng, L., Zhang, A., Pei, T., 2020. Evaluating the cumulative and time-lag effects of drought on grassland vegetation: A case study in the Chinese loess plateau. J. Environ. Manag. 261, 110214 https://doi.org/10.1016/j.jenvman.2020.110214.

Zhu, Z., Zhou, Y., Seto, K.C., Stokes, E.C., Deng, C., Pickett, S.T., Taubenböck, H., 2019. Understanding an urbanizing planet: strategic directions for remote sensing. Remote Sens. Environ. 228, 164–182. https://doi.org/10.1016/j.rse.2019.04.020.

Zink, M., Samaniego, L., Kumar, R., Thober, S., Mai, J., Schäfer, D., Marx, A., 2016. The German drought monitor. Environ. Res. Lett. 11 (7), 74002. https://doi.org/10.1088/1748-9326/11/7/074002.